Image Process Discharge Classification under Nonuniform Fields in Air and He at Low Pressure

M. Hikita M. Fujimori N. Hayakawa
and H. Okubo

Nagoya University, Nagoya, Japan

ABSTRACT

This paper described the discharge classification under nonuniform electric field in air and He at low gas pressures for the application of HV technology to the power apparatus in space. In order to discuss quantitatively the change of the discharge, an image processing method was introduced. In the first place, 4 shape parameters were proposed to characterize the discharge pattern: the area S_H, the flatness rate H/V, the location g of the center of luminosity of the luminous area, and the length L of the positive column. The analysis with the image processing for air revealed that S_H, H/V and g continuously increased as the pressure decreased. Consequently, the discharge type in air was successfully classified into 3 regions with two boundary pressures 200 and 2000 Pa over the pressure range from 1.3×10^4 to 27 Pa. The discharge in He was also analyzed in the same way. Another parameter, the effective current density J_e, was introduced, which was defined as a ratio of the discharge current to the luminous area viewed from the vertical direction. J_e proved to be independent of the discharge current I_d, so that there is the possibility that J_e was suggested as a universal parameter to classify the discharge in a nonuniform electric field in vacuum.

1. INTRODUCTION

SINCE space technology has been developing remarkably, application of HV technology in space is now underway [1–4]. For instance, the technology for large power generation and transmission in space stations is receiving special attention. In this case, electrical insulation will play a decisive role in reliable operation of the power apparatus in space.

In particular, the understanding of discharge characteristics in space environment is crucial for the application of HV technology to the power apparatus. The space environment is characterized by severe, unique conditions such as low to ultra high vacuum, no gravity, wide temperature difference, UV radiation, plasma, magnetic field, *etc.* [5–7]. For example, surface discharge due to charging of solid dielectrics in space caused failure of several satellites. In such special circumstances, the terminology defined conventionally in the field of gas discharge technology may no longer be used: the definition of arc, glow and corona discharges. Even the wrong terminology concerning discharges is sometimes used.

There have been extensive studies of discharge phenomena in vacuum simulating the space environment [8, 9]. The theory of discharges at low gas pressures has been established for uniform and quasi-uniform electric fields [10]. However, it is impossible to apply directly uniform field theory to nonuniform field discharge phenomena. Consequently, the mechanism of discharges under

1070–9878/95/ $3.00

nonuniform electric field in vacuum is not sufficiently clarified, especially discharges in low pressure He which is dominant in some regions of high altitude space. From the above points of view, we have been investigating discharge phenomena in low, medium and high vacuum simulating the space environment. For the investigation of discharge phenomena, a spectrum analysis of the emitted light is regarded as a useful method [11]. However, under the nonuniform electric field, the shape of discharge depends on the pressure and the kind of gases. Thus, it is important to recognize the shape of discharge for the elucidation of discharge mechanism in space environments. In the first step, in this paper, an attempt is made to classify the discharge type in vacuum of air and He under nonuniform electric field. For this purpose, the image of the discharge shape in vacuum is recorded with a video camera and analyzed by means of an image processing technique.

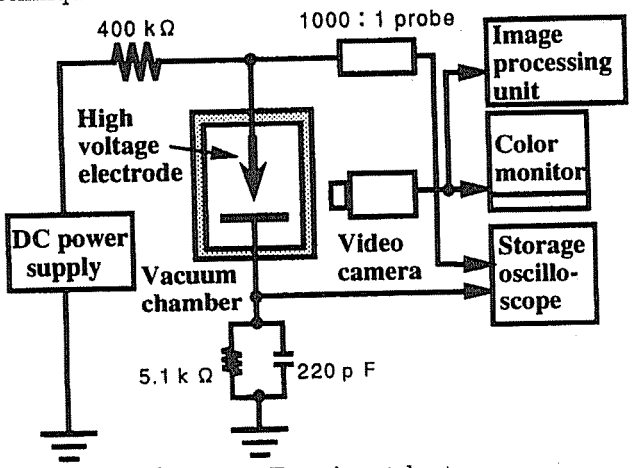

Figure 1. Experimental setup.

2. EXPERIMENTAL

Figure 1 illustrates the experimental setup, which consists of a vacuum chamber made of glass, a dc power supply, a video camera, a color monitor and an image processing unit. The point-plane electrodes (point radius of the curvature is 50 μm) were placed in the vacuum chamber. After evacuation to $\sim 10^{-1}$ Pa, air or He was introduced and the chamber back filled to atmospheric pressure. Then, the pressure was set at a given value between 0. 1 MPa and 0.1 Pa. A dc ramp voltage with positive polarity was applied to the HV electrode at a rate of 0.1 kV/s. Discharge phenomena were observed with a video camera and recorded on a video tape. The recorded data were used for image processing to quantify the discharge pattern and classify the discharge type. The image processing unit has the resolution of 512×512 pixels per image, and one pixel can have 256 values of light intensity. All measurements were performed at room temperature.

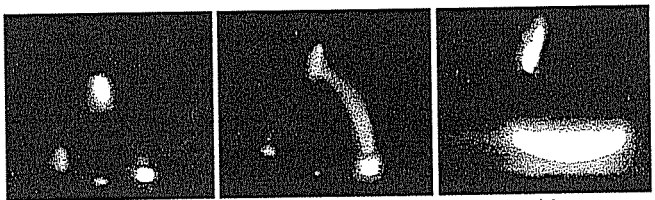

Figure 2.

Pictures of observed discharge pattern in air for different pressures with the needle-plane electrode configuration and the gap length d = 15 mm by applying positive dc voltage. (a) 1.3×10^4 Pa, I_d = 5.9 mA. (b) 1.3×10^3 Pa, I_d = 0.78 mA. (c) 130 Pa, I_d = 0.78 mA.

3. CHANGE OF DISCHARGE TYPE IN VACUUM

Figures 2(a) to (c) show pictures of observed discharge pattern in air at 1.3×10^4, 1.3×10^3, 130 Pa, respectively, for the needle-plane electrode configuration with the gap length d = 15 mm. As seen from the picture (a), at 1.3×10^4 Pa, glow discharge takes place with emitting light only at the electrode edge. When the pressure decreases to 1.3×10^3 Pa (b), a positive column begins to emerge. Further decrease of the pressure to 130 Pa (c) causes the positive column to disappear again and the luminous part of discharge to start spreading horizontally along the plane electrode. The discharge type of the luminous part is considered to correspond to negative glow [12]. At 27 Pa, although not shown in Figure 2, the glow discharge eventually diffused in the form of a plane and moved to the vicinity of the needle electrode edge.

To summarize the results, there were two major features in the change of the observed discharge type: With decreasing pressure, the size of the negative glow floating above the plane electrode increased, the shape was getting flat, and it approached the upper needle electrode, and the positive column emerged and disappeared again with decreasing pressure.

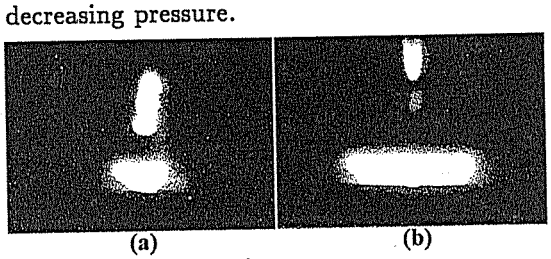

Figure 3.

Pictures of discharge in air at 270 Pa for different discharge currents I_d. The other conditions were the same as those in Figure 2. (a) I_d = 0.39 mA. (b)I_d = 2.0 mA.

On the other hand, the discharge type was found to change with the discharge current I_d. Figures 3(a) and

(b) depict pictures of discharge in air at 270 Pa for I_d = 0.39 and 2.0 mA, respectively; the other conditions were the same as those in Figure 2. It is evident from the Figures that as I_d increases from 0.39 to 2.0 mA, the negative glow above the plane electrode begins to diffuse in the horizontal direction and the positive column disappears. Other experiments allowed us to confirm that the manner of the change of the discharge type in air with I_d was similar to that observed at 270 Pa.

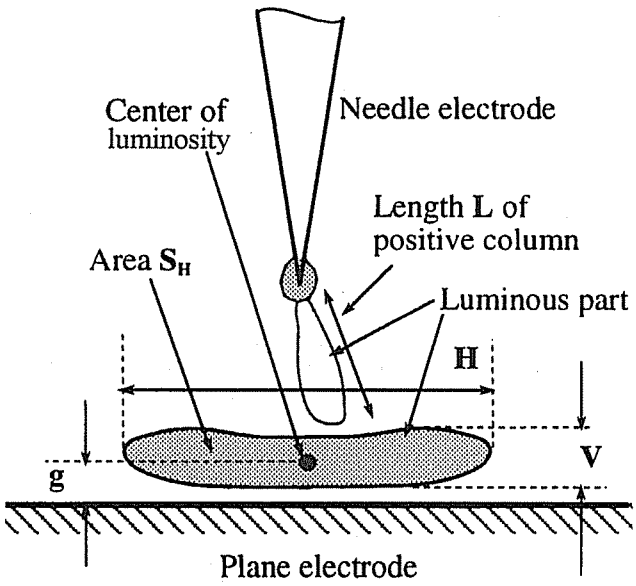

Figure 4.

Illustration of four new shape parameters to characterize the discharge type.

4. APPLICATION OF IMAGE PROCESSING TO DISCHARGE TYPE CLASSIFICATION

In order to quantitatively discuss the change of the discharge shape obtained above, the image processing method is introduced [13]. Let us introduce 4 shape parameters to characterize the discharge type as illustrated in Figure 4: the area S_H, the flatness rate H/V, the location g of center of luminosity for the luminous part ($g = 0$ on the plane electrode) and the length L of positive column. H and V are, respectively, the maximum width and maximum height of the luminous part parallel to and perpendicular to the plane electrode, g is the location between the center of luminosity and the plane electrode, and S_H is the cross sectional area of the discharge viewed from the horizontal direction. Note that the three parameters S_H, H/V and g are concerned with the discharge appearing above the plane electrode.

Figure 5 shows the image processing procedure from a given original image to a binary image. It should be noticed, as seen in the Figure, that the binary conversion is eventually performed for one of the components R (Red), G (Green) and B (Blue). Firstly, an original image is taken to the image processing unit through the video camera. After the color image is decomposed into R, G and B components, the intensity of each component is divided by 3 for convenience. Secondly, the image thus obtained is converted into one of the three components R, G and B, and then the intensity of one unmodified component and two modified ones are summed up. Note that this is a simple addition without any filter calibration. In Figure 5, as an example, R and B components are converted into G component. Hence, an image reduced to one component (a green scale image in Figure 5) is obtained. The next step is the binary conversion of the monotone image. One has to determine a threshold level of light intensity for the binary conversion. In the present work, after comparing discharge shapes before and after the binary conversion, 70% of the maximum intensity is taken as the critical one. The shape feature measurement for the binary image allows the calculation of the 4 shape parameters on discharge type.

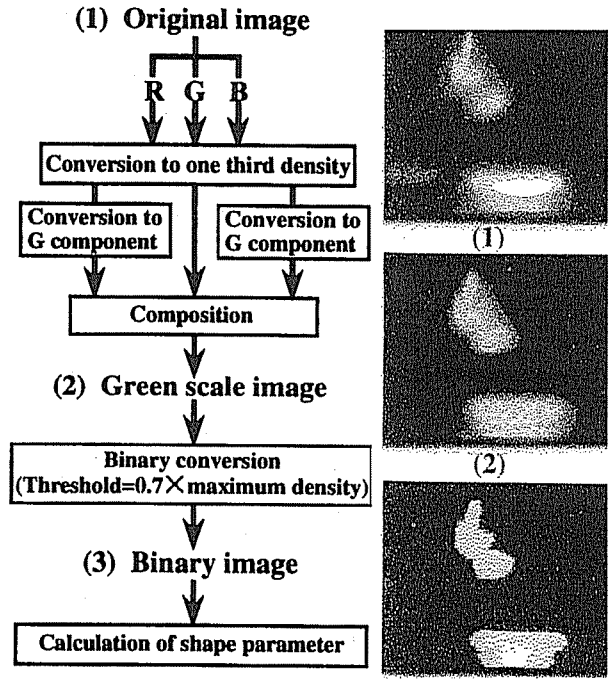

Figure 5.

Image processing procedure from a given original image to a binary image.

Figure 6 shows the area S_H of discharge and the flatness rate H/V as a function of gas pressure in air for different gap lengths d with positive dc voltage application. Dotted lines represent the two threshold pressures of 2000 and 200 Pa to classify the discharge. It is seen that S_H and H/V begin to rise with decreasing pressure.

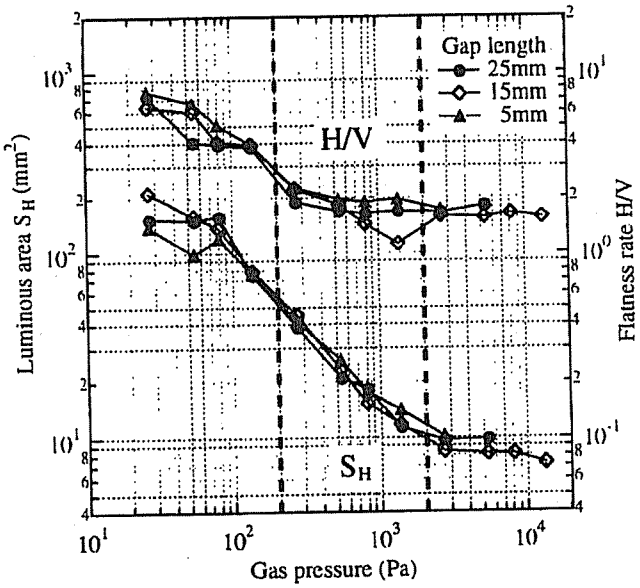

Figure 6.

Gas pressure dependence of the area S_H and the flatness rate H/V of the luminous part of discharge in air for different gap lengths d for positive dc voltage.

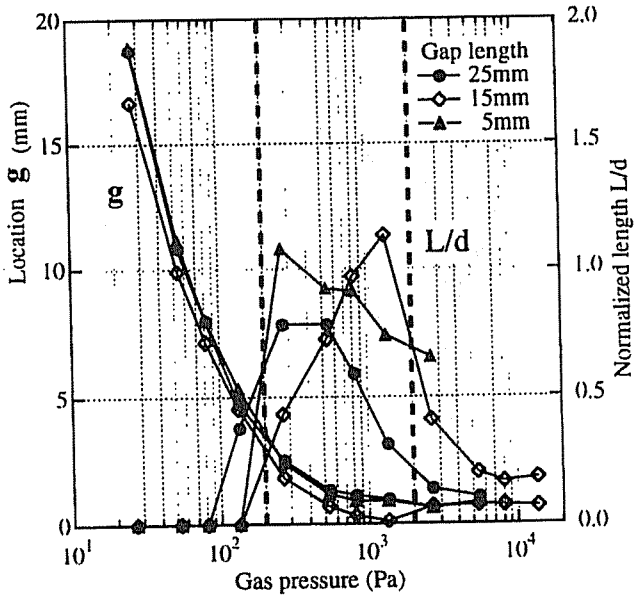

Figure 7.

Gas pressure dependence of the location g of the center of luminosity and the normalized length L/d of the positive column in air.

S_H and H/V exhibit the critical pressure, respectively $\sim$ 2000 and 200 Pa, at which there exists a change in the first order derivatives of S_H and H/V with respect to the pressure. In other words, the above results indicate that the discharge type can be divided into three regions with two threshold pressures 2000 and 200 Pa under the present experimental conditions. It should be also noted that the two curves S_H and H/V *vs.* gas pressure are independent of the gap length.

Figure 7 shows the gas pressure dependence of the location g of center of luminosity and the normalized length L/d of the positive column in air; the experimental conditions are the same as given in Figure 6. Note that the length L of the positive column is normalized by each gap length d. g sharply rises as the pressure decreases from $\sim$ 200 Pa, as does H/V. The result implies that the negative glow approaches the needle electrode with a reduction of the pressure. g is also independent of the gap length. On the other hand, although the length L/d of the positive column changes with the gap length, the pressures at which the positive column emerges and disappears again are almost the same values for different d: 2000 and 200 Pa, respectively. Consequently, the image processing technique employed here allowed us to classify successfully the discharge in air into 3 regions in the pressure range from 1.3x10^4 to 27 Pa.

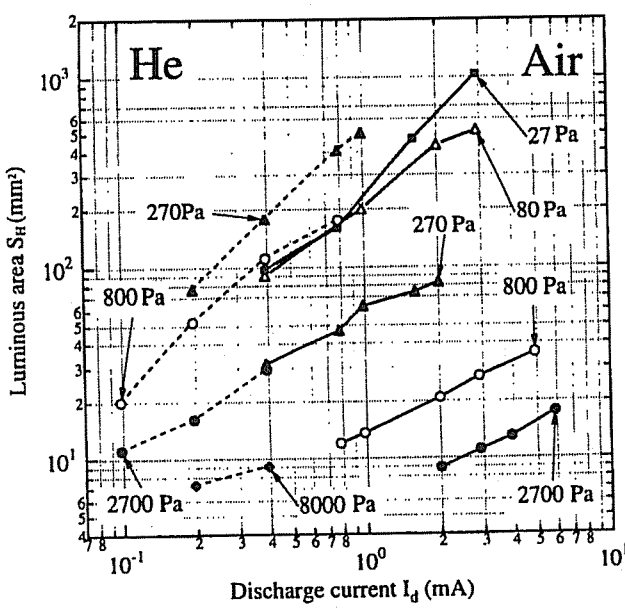

Figure 8.

Relationship between area S_H and discharge current I_d for different gas pressures in air and He gas with gap length 15 mm for applying positive dc voltage.

5. COMPARISON OF DISCHARGE TYPE BETWEEN AIR AND He IN VACUUM

As shown in Figure 3, the discharge type also varied with the discharge current I_d. Figure 8 shows the rela-

tionship between S_H and I_d for different pressures in air (solid lines) and He (dotted lines) with $d = 15$ mm. It is obvious that S_H increases with a rise of I_d at a constant gas pressure for both gases, and that S_H also increases as the pressure goes down. The image processing of the discharge also revealed that H/V for both air and He exhibited similar characteristics with a variation of the gas pressure and I_d as S_H did. It was also found that g was almost independent of I_d for a given pressure for both air and He. As the pressure decreased, g rose, indicating that the negative glow was approaching the needle electrode.

It should be noticed that the positive column in He did not appear under the present conditions; this result remarkably differed from that in air. Consequently, it has been shown that although the values themselves of three shape parameters S_H, H/V and g are different by one order of magnitude between air and He at the same pressure, the manner the three parameters change with I_d and gas pressure is similar in the two gases.

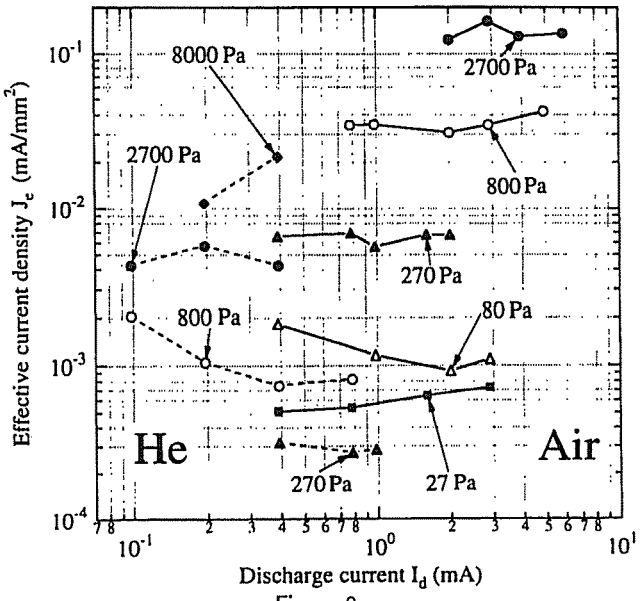

Figure 9.

Relationship between the effective current density J_e and discharge current I_d for different gas pressures in air and He gas.

In addition, to discuss in more detail the classification of the discharge type observed in low and medium vacuum under nonuniform field, another new shape parameter J_e, the effective current density, is introduced. Let us define J_e as in (mA/mm^2)

$$J_e = \frac{I_d}{S_V} \tag{1}$$

where $S_V = \pi(H/2)^2$, is the cross section area of the luminous part of discharge viewed from the normal direction. Figure 9 shows the effective current density J_e as a function of discharge current I_d in air and He for different pressures. The symbols are the same as those in Figure 8. As seen in the Figure, J_e is almost independent of I_d for a given constant pressure and is nearly proportional to the pressure. This indicates that the luminous area S_V of discharges increases with I_d. With the obtained results, the discharge may be in the first stage glow or the normal glow [12] within the present conditions. It is useful to determine the equivalent current density even though it is a nonuniform field. Because of being independent of I_d, J_e can be a more universal parameter to classify the discharge in comparison with the other preceding shape parameters. Hence, there is the possibility that the use of J_e allows one to predict the gas pressure of a discharge in a known gas, or to identify the gas components from a known pressure. The image processing technique will be a powerful and useful means to construct a database of discharge shape for various gases and, as a result, to classify the discharge. Further investigation is necessary on the quantitative classification of discharge in He and on the relationship between discharge mechanisms and the shape parameters derived from the image processing.

6. CONCLUSIONS

FOR the development of space technology, an attempt was made to quantify the pattern of the luminous part of discharge in vacuum using an image processing technique. As an example, the image processing was applied to classify discharges in low and medium vacuum for air and He under dc nonuniform electric fields. In the first place, 4 shape parameters were introduced to characterize the discharge shape: the area S_H, the flatness rate H/V, the location g of the center of luminosity of the discharge luminous part, and the length L of the positive column. The analysis with the image processing for air revealed that S_H, H/V and g continuously increased as the gas pressure decreased. It was also found that they were almost the same value, irrespective of the gap length of 5, 15 and 25 mm. Consequently, the discharge was successfully classified into 3 regions with two boundary pressures 200 and 2000 Pa over the pressure range from 1.3×10^4 to 27 Pa. The effective current density J_e was also introduced, which was defined as a ratio of the discharge current I_d to the cross section area of the luminous part viewed from the vertical direction. It was pointed out that J_e can be a more universal parameter to identify the discharge type in vacuum for air and He than the preceding 4 shape parameters.

REFERENCES

[1] M. F. Rose, "Power Technology for Space Systems", 6th Int. Symp. HV Eng. 45. 01, 1989.

[2] M. Gollor and K. Rogalla, "High Voltage Design of Vacuum-insulated Power Supplies for Space Applications", IEEE Trans. on Elect. Insul., Vol. 28, pp. 667–680, 1993.

[3] H. M. Banford, M. J. Given and D. J. Tedford, "A Space Simulation Chamber for Space Power Insulation", IEEE Int. Symp. on Elect. Insul., pp. 24–27, 1992.

[4] R. E. Quigley Jr. and L. D. Massie, "Future Trends in Space Power Technology", 26th IECEC, Vol. 2, pp. 1–7, 1991.

[5] E. Szuszczewicz, "The Ionospheric Environment: Understanding, Predictability and Influences on Satellite and Communication Systems", 28th Aerospace Sciences Meeting, AIAA-90–0288, 1990.

[6] D. C. Wilkinson, "Trends in Spacecraft Anomalies", Proc. Spacecraft Charging Technology Conference 1989, p. 1, 1991.

[7] M. Lauriente and H. B. Garrett, "A Space Environment Data Resource", Proc. Spacecraft Charging Technology Conference 1989, p. 556, 1991.

[8] G. G. Karady, M. D. Sirkis and J. R. Oliva, "Degrading Effect of High-altitude Corona on Electronic Circuit Boards", IEEE Trans. on Elect. Insul., Vol. 26, pp. 1216–1219, 1991.

[9] M. F. Rose, "Insulation and Discharge Phenomena in the Space Environment", XVth Int. Symp. on Discharges and Elect. Insul. in Vacuum, pp. 547–554, 1992.

[10] F. L. Jones, "Ionization Growth and Breakdown", Encyclopedia of Physics, *Gas Discharges*, pp. 21–26, Springer-Verlag, 1956.

[11] M. Komatsubara, M. Ishii and E. Tsumura, "Research on Outgas and Light Emission from Electrostatic Discharge on Polymer Films in Vacuum", Trans. IEE Japan, Vol. 114-A, No. 7/8, pp. 528–534, 1994.

[12] Y. P. Raizer, *Gas Discharge Physics*, pp. 167–171, Springer-verlag, 1991.

[13] E. L. Hall, *Computer Image Processing and Recognition*, Academic Press, 1979.

This paper is based on a presentation given at the 16th International Symposium on Discharges and Electrical Insulation in Vacuum, Moscow, Russia, 1994.

Manuscript was received on 19 August 1994, in final form on 23 January 1995.